# Fractal study of magnetic domain patterns

Bao-Shan Han,[1,*] Dan Li,[1] De-Juan Zheng,[2] and Yan Zhou[1]
[1]*State Key Laboratory of Magnetism, Institute of Physics, Center of Condensed Matter Physics, Chinese Academy of Sciences, Beijing 100080, China*
[2]*Technical Institute of Physics and Chemistry, Chinese Academy of Sciences, Beijing 100080, China*
(Received 27 February 2002; published 19 July 2002)

Fractal geometry is introduced into the analysis of ''two-phase'' magnetic domain patterns. The line-measuring dimension $D_{line}$ is selected to quantitatively describe the ''line structure'' patterns of the multi-branched domains (MBD's) formed in garnet bubble films, and a meaningful $D_{line}$ can be related to the numbers of vertical Bloch lines in their walls, i.e., to the hardness of the MBD's. For quantitatively describing the ''plane-filling'' domain patterns of magnetic materials with uniaxial anisotropy, such as corrugation and spike, even ''flower,'' domains, the box-counting dimension $D_{box}$ is selected. For describing the series of domains of Co and Dy-NdFeB single crystals due to branching process, $D_{line}$ and $D_{box}$ are used in section. Our results show that two phase domain patterns possess fractal natures, and can be described by fractal dimensions.

DOI: 10.1103/PhysRevB.66.014433 PACS number(s): 75.70.Kw, 61.43.Hv, 75.60.Ch

The concept of ''fractal'' was proposed by Mandelbrot in 1975.[1] Since the 1980s, fractal study has become a rapidly developing field, and has been applied in a variety of disciplines.[2,3] Fractal is closely related to nonlinear phenomena, and is appropriate to analyze irregular and fragmented patterns; therefore, the fractal dimension $D$ is a better parameter to describe them quantitatively. In condensed-matter physics, fractal study has mainly concentrated on growing dynamics to describe the variation of patterns with temperature and time, etc.

The existence of magnetic domain patterns is a common phenomenon in ferromagnets. They may exist to reduce stray field energies, or to the adapt to local anisotropy or sample shape, depending on the material parameters and the sample size. Actually, all these energies are nonlinear functions in space, and magnetic domain patterns result from their balance. Therefore, magnetic domain patterns should possess a fractal nature.

In the field of magnetic domains, cellular domain patterns as self-organizing critical systems have been discussed.[4,5] But this discussion was limited to simple cellular patterns. In this paper, fractal study will first be introduced into the analysis of ''two-phase'' complicated magnetic domain patterns.

The intermediate states of the first kind of superconductor and uniaxial ferromagnets are famous examples of a two-phase domain structure. In this paper we analyze two-phase magnetic domain patterns of uniaxial ferromagnets in two cases. The first case concerns multibranched domains (MBD's) in garnet bubble films, formed under nonlinear bias-pulsed fields and in a finite space. The second case concerns two-phase magnetic domain patterns formed by a branching process along the easy axis direction in uniaxial ferromagnetic plates with infinite dimensions. In the above two cases, we have found the existence of fractal natures, and introduced appropriate fractal dimensions to describe their self-similarity and scale invariance in a statistical sense.

The Bloch walls of stripe domains in bubble films go through the film thickness perpendicularly, and separate the ''black'' and ''white'' domains with upward and downward magnetizations, respectively. It was proposed that a single round-shaped MBD could be formed inside a pancake coil with 1 mm inner diameter under the joint application of a bias field $H_b$ and a bias rectangular pulse field $H_p$.[6] In fact, MBD's were formed during a rapid drop ($\sim$60-ns falling time) of $H_p$; thus the formation of MBD's is associated with a nanosecond nonlinear process in a finite space. With a decrease of $H_b$ from $H[d]$ (which is called the ''critical static bias field for multibranched expansion'' because a multibranched expansion cannot occur if $H_b > H[d]$ for bubble films) the dynamically compressed bubble suffers a larger and larger rapid drop of $H_p$ $[(H_b + H_p) = \text{const.}]$ during its falling time, resulting in a more and more complicated patterns of MBD with more and more vertical Bloch lines (VBL's) excited in their walls inside a pancake coil. In other words, the patterns of MBD's are related to the numbers of VBL's in their walls, i.e., the hardness of the MBD's. In the experiment, the formed MBD were contracted and classified into a type of hard domains. [There are three types of hard domains in bubble films, i.e., ordinary hard bubbles (OHB's) and the first and second types of dumbbell domains (ID and IID), and in their walls the numbers of VBL's are successively increased in the order OHB$\rightarrow$ID$\rightarrow$IID.[7]] Therefore, on the one hand, we intend to use the fractal dimension to describe the MBD pattern quantitatively; on the other hand, by means of the statistical formation of MBD's,[6] the curve of $D$ vs $H_b$ can also be related to the excitation of VBL's in the walls of MBD's.

In our experiments, by using a transition polarizing microscope (Faraday effect observation), 70 photos of MBD's and a few soft bubble (SB's, i.e., normal bubbles) were taken at 12 $H_b$'s for sample No. 1 with a nominal composition of $(YSmCa)_3(FeGe)_5O_{12}$.[6] For the fractal study, these photos need to be processed. As an example, Fig. 1(a) is the photo of a typical MBD, in which the inner edge of the 1-mm id pancake coil is partially and faintly shown by the black area at the four corners, and the round-shaped ''white'' MBD is surrounded by the ''white'' stripe domains intruding into the

 

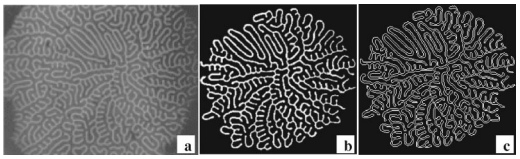


FIG. 1. (a) Photo of a typical MBD, formed at the static bias field $H_b=(44.0/4\pi)$(kA/m), and contracted into an IID with a collapse field $H_{col}=(93.6/4\pi)$(kA/m). (The photo length is about 0.9 mm) (b) Dual value description of this MBD (figure sizes: 517 $\times$480 pixels) (c) Dual boundary description of this MBD (517 $\times$480 pixels).

coil. The steps of the image processing involved (1) ''wiping'' away all irrelevant ''white'' domains; (2) raising the contrast between the ''white'' MBD (with downward magnetization) and the ''black'' domains (with upward magnetization) around it by means of ''dual value'' processing, as shown in Fig. 1(b); (3) adopting a ''dual boundary method,'' i.e., extracting all the pixel points on both sides of each branch, resulting in a ''dual boundary description'' of MBD's, as shown in Fig. 1(c).

Figures 2(a)–2(d) typically show a SB and three MBD's formed at different $H_b$ in a dual-value description (480 $\times$580 pixels). Three MBD's were contracted into OHB, ID, and IID, respectively. In the fractal study of image patterns, the usual way is to calculate their box-counting dimension ($D_{box}$). However, the patterns in Figs. 2(a)–2(d) are characteristic of a ''line'' structure. Apparently, they cannot be described by $D_{box}$. After comparison, a ''line-measuring dimension'' $D_{line}$ was selected.

The definition of $D_{line}$ is

$$D_{line}=-\lim_{\delta\to 0}\frac{\ln[L(\delta)]}{\ln\delta}. \tag{1}$$

Before calculating $D_{line}$, in order to obtain the domain wall curve the patterns in a dual-value description [e.g., in Figs. 2(a)–2(d)] should be converted to that in a ''dual boundary description.'' An example is shown in Figs. 1(b) and 1(c). In this way, in the calculation of $D_{line}$, the running direction of a domain curve is unique at every point. This method is of significance not only in mathematics but also in physics, because the boundary of ''white'' and ''black'' domains is actually the domain walls of MBD's.

The procedure to calculate $D_{line}$ starts from measuring the length of a curve by using a ruler of length $\delta$. By changing the ruler $\delta$ to measure the wall curve length $L(\delta)$ and carrying out a linear regression to the curve of $\ln L(\delta)$ vs $\ln(\delta)$ (called the ''fractal curve'' below), $D_{line}$ is obtained.

The corresponding fractal curves of Figs. 2(a)–2(d) are shown in Figs. 2(e)–2(h). As shown in Fig. 2(a), the ''single-branch'' domain with only one ''head'' and one ''tail'' is a SB. But the patterns of OHB's, as typically shown in Fig. 2(b), are characteristic of a few long curved branches and comb teeth. For the ID [Fig. 2(c)], they have many long branches and more comb teeth growing from some long branches. For the IID [Fig. 2(d)], the number of long branches is large, and lots of comb teeth were grown from almost each long branch. It is obvious that with decrease of $H_b$ from $H[d]$, the successive appearance of OHB's, ID's, and IID's, i.e., the hardening process of MBD's, is certainly associated with the growth and quantity increase of long branches and comb-teeth.

It is seen in Figs. 2(e)–2(h) that the four fractal curves consist of three segments. On the first segment ($\ln\delta<2.6$), the calculated $D_{line}$ is all about 1.05, indicating that this segment is not characteristic due to rulers that are too short. However, for the second one ($\ln\delta\sim 2.6$–$4.5$), $D_{line}$ is evidently increased in the order OHB$\rightarrow$ID$\rightarrow$IID, indicating that this segment is characteristic of MBD patterns. It also manifests that the rulers ($\delta\sim 14$–$90$) used, and their corresponding lengths ($\sim 20$–$110$ $\mu$m), well match with the length of comb teeth and the bending parts of the long branches, so that $D_{line}$ can reflect their growth and quantity. In fact, the existence of the scale invariance of MBD patterns has been confirmed by the linearity of the second segment. Finally, the third one ($ln\ \delta>4.5$) should be cut off because the patterns are too curved to be correctly measured by straight long rulers.

The average values of $D_{line}$ were calculated for all photos taken at $12H_b$'s, and the curve of $D_{line}$ vs $H_b$ is shown in Fig. 3. The error of $D_{line}$ mainly comes from the determination of the characteristic segment and its linear regression,

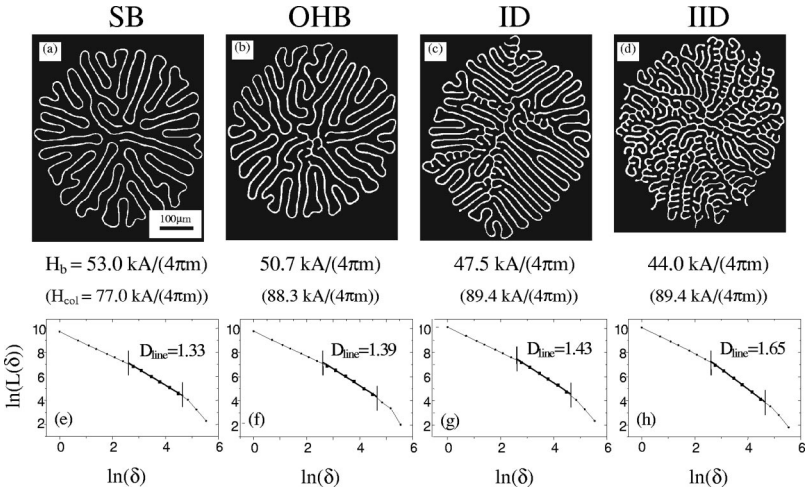


FIG. 2. Typical patterns of a single-branch domain and three MBD's in a dual-value description (480$\times$580 pixels), and their corresponding fractal dimension measurement curves. (a) Single-branch domain, which was contracted into a SB. (b) MBD, OHB. (c) MBD, ID. (d) MBD, IID. The static bias field $H_b$, at which they were formed, and their collapse fields $H_{col}$ are marked. (e)–(h) the corresponding fractal curves of the domain patterns in (a)–(d). The $D_{line}$ values calculated on the second segment are marked. Sample No. 1, $H[d]=(55.0/4\pi)$(kA/m), at room temperature.

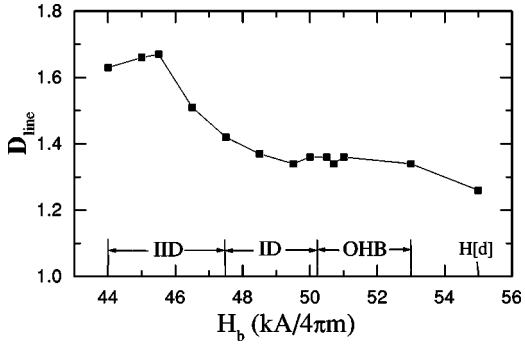


FIG. 3. The line-measuring dimension $D_{line}$ of the MBD of sample No. 1 as a function of the static bias field $H_b$, at which they were formed. The critical static bias field $H[d]=(55.0/4\pi)\times$(kA/m) for the multibranched expansion, and the main regions of $H_b$ for the formation of OHB's, ID's, and IID's are marked.

and was estimated to be 0.03–0.05 for most $H_b$. For analysis, the formation regions of OHB, ID, and IID (Ref. 6) were marked in Fig. 3 to illustrate that the variation of $D_{line}$ is also related to the excitation of VBL's in the walls of MBD's.

It is seen in Fig. 3 that with decrease of $H_b$ from $H[d]$, $D_{line}$ is slightly increased over the formation region of OHB's, because the pattern difference between OHB's and SB's is small. However, while $H_b$ is decreased into the ID region, $D_{line}$ is gradually increased. But when $H_b$ is decreased into the IID region, the $D_{line}$ is steeply increased. Thus $D_{line}$ seems a better parameter to quantitatively describe the MBD patterns, in particular the IID patterns. This fact means that the hardness of the IID walls is remarkable. We believe that this is associated with the remarkable static characteristics of IID.[7]

The second case deals with the branching process of two phase domains along the easy axis direction in uniaxial ferromagnetic plates of infinite dimensions. The theory of two-phase domain branching was proposed early by Landau[8] and Lifshitz,[9] then developed by Hubert.[10] In their theories, the geometric property of two-phase domains was described by the ''domain width'' *w*: For thinner crystals, *w* increases following a $t^{1/2}$ law, i.e., w $\sim\sqrt{t\gamma_w}$, and the domain wall energy density $\gamma_w$ can be calculated by measuring *w* for given *t*. But for thicker crystals, *w* increases following a $t^{2/3}$ law, i.e., $w \sim t^{2/3}$. Moreover, the thickness corresponding to the crossover of the two power laws is defined as the critical thickness $t_s$.[11] However, *w* is better for the simple domains, such as stripe, parallel plate, etc., in which the straight Bloch walls are perpendicular to sample surface, and go through the whole thickness. But for the complicated surface domains of the materials with a uniaxial anisotropy, the concept of ''domain width'' becomes faint. In fact, for these materials, with an increase of *t*, branching, tilting, curving, and domain refinement toward the surface occur gradually, which causes the domain walls to no longer go through the whole thickness. As a result, the domain patterns in surface layer vary gradually from simple to complicated, leading to the appearance of corrugation and spike domains, even to the most complicated ''flower'' domains.

Due to the fact that the complicated domain patterns in surface layers are entirely different from the simple ones at the interior of the crystals, in Ref. 11 the ''surface domain width'' $w_s$ and the ''basic domain width'' $w_b$, were used to describe them, respectively. However, as discussed above, the complicated surface domains result from the ''basic'' domains along the easy axis by the nonlinear branching process, such as ''two branching,'' ''three branching,'' etc. Actually this is a fractal process in space; thus the resultant domain patterns should possess a fractal nature, i.e., self-similarity and scale invariance. Although the fractal nature of the domain branching process was pointed out by Hubert,[11] we have used ''fractal dimension'' to quantitatively describe the variation of domain patterns from simple to complicated, and to distinguish the complicated patterns in different materials.

In fact, the domain walls of complicated domains are a combination of Bloch walls and Néel walls, and the wall energy density is a multivariable nonlinear function. With the branching process, the domain walls sequentially vary from two (2D) to three dimensional (3D) toward the surface along the easy axis, while the domain patterns on surface layer vary from 1D to 2D. Now the question is how to use fractal dimensions to describe the above branching process and the variation of surface domains. For reaching this goal, it is crucial to acquire some series of reliable surface domain patterns of different magnetic single crystals with various thicknesses *t* ranging from small to very large. Fortunately, two series of domain patterns (Kerr effect observation) on the basal plane of Co single crystals and Dy-modified NdFeB are available in Figs. 5.4 and 5.5 of Ref. 11, respectively. The fractal dimension and its variation with *t* were calculated as follows.

In Ref. 11, the patterns of Figs. 5.4(a) ($t\sim 0-5$ $\mu$m) and 5.5(a) ($t\sim 1-14$ $\mu$m) for thinner crystals are essentially in a ''line'' structure. Therefore, similar to the stripe domains in bubble films, $D_{line}$ was calculated. Considering that in these two photos the ''line'' structure patterns are still gradually changed with an increase of *t*, Figs. 5.4(a) and 5.5(a) in Ref. 11 were reasonably split into four pieces to obtain more data points. However, for thicker crystals the patterns of Figs. 5.4(b)–5.4(d) ($t\sim 18$, 50, and 400 $\mu$m) and Figs. 5.5(b)–5.5(d) ($t\sim 40$, 120, 600 $\mu$m) in Ref. 11 are characteristic of ''plane filling;'' therefore, the box-counting dimension $D_{box}$ was calculated.

As examples, the ''flower'' patterns of the thickest Co and Dy-NdFeB crystals [Figs. 5.4(d) and 5.5(d) of Ref. 11] were copied in Figs. 4(a) and 4(b) of this paper, and their corresponding fractal curves calculated are shown in Figs. 4(c) and 4(d), respectively. Apparently, these two fractal curves are similar, and all consist of two data segments with different slope. Taking the fractal curve of Dy-NdFeB [Fig. 4(d)] as an example, in its second segment ($\ln\delta>3.0$) the calculated $D_{box}=2$ is actually the dimension of the whole image plane; thus this segment should be cut off. In the first segment ($\ln\delta<3.0$) with smaller $\delta$, the calculated $D_{box}=1.65$ is thus meaningful to describe this domain pattern. In the same way, from the first segment of the fractal curve of Co crystal [Fig. 4(c)], the calculated $D_{box}=1.55$. We believe that the linearity of the first segment is a confirmation of the exis-

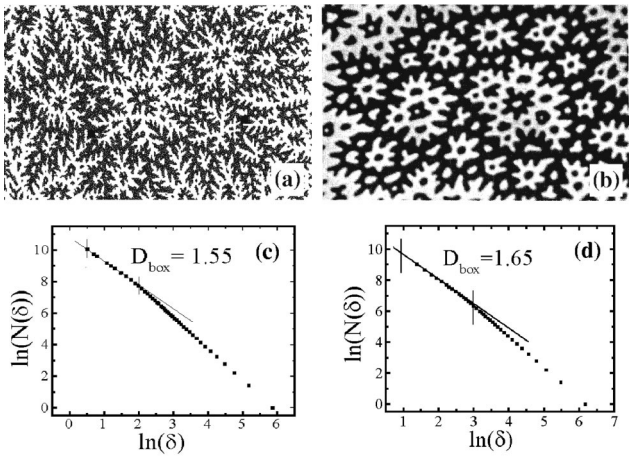


FIG. 4. The ''flower'' patterns on the basal plane of the thickest Co (a) and Dy-NdFeB (b) crystals [quoted from Figs. 5.4(d) and 5.5(d) of Ref. 11, respectively]. The photo sizes are about 29 $\times 17$ $\mu$m). Their corresponding fractal curves are shown in (c) and (d), respectively.

tence of self-similarity and scale invariance. In fact, the ''flower'' domain patterns in both Figs. 4(a) and 4(b) are in the metastable state by a self-organizing critical system, resulting from a full branching process in a very thick Co crystal ($t=400$ $\mu$m) and a Dy-NdFeB crystal ($t=600$ $\mu$m), respectively.

After the calculation of $D_{line}$ and $D_{box}$ for the domain patterns of Co and Dy-NdFeB crystals, their curves of $D$ vs $\log t$ were obtained. Then the thickness, corresponding to the maximum of the curve $\partial D/\partial \log t$ vs $\log t$, was defined as a critical thickness $t_c$, which is actually the turn point for the transition of domain patterns from simple to complicated. The calculated $t_c$'s for Co and Dy-NdFeB are 3.7 and 10 $\mu$m, respectively. As a result, their normalized curves of $D$ vs $\log(t/t_c)$ are shown in Fig. 5. These two curves indicate the following. (1) $D_{line}$ and $D_{box}$ can describe the complexity degree of the ''line'' structure and ''plane filling'' patterns, respectively. (2) The variation of domain patterns with $t$ can be quantitatively expressed by $D_{line}$ and $D_{box}$ in sections. Furthermore, when $t/t_c$ is increased to several tens, $D$ approaches a saturated value $D_{sat}$, which means that the domain patterns in a surface layer finally become fixed. Actually, a saturated dimension $D_{sat}$ and its corresponding ''flower'' patterns are characteristic of different materials. In particular, we think that the ''flower'' patterns seem to be ''finger print'' of the materials.

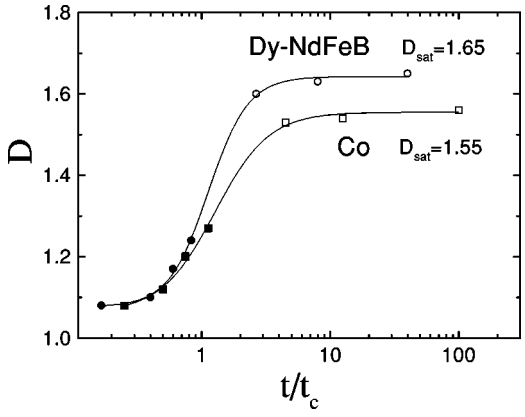


FIG. 5. The fractal dimension $D$ as a function of the normalized thickness $t/t_c$, calculated from two series of domain patterns of Co (square) and Dy-NdFeB (circle) single crystals, shown in Figs. 5.4 and 5.5 of Ref. 11, respectively. Solid and empty squares or circles represent $D_{line}$ and $D_{box}$, respectively.

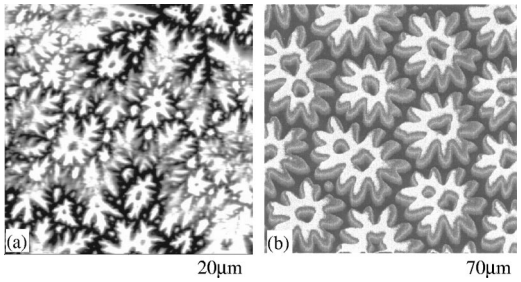


FIG. 6. The ''flower'' domain patterns taken by using MFM on the surface layer of (a) a thick $NdFe_{10.5}Mo_{1.5}$ single crystal and (b) a 60-$\mu$m-thick magnetic garnet film (quoted from the ''Magnetic Force Microscopy Image Book,'' DI, 1995).

In order to study the correlation between $D_{sat}$ and material parameters, in addition to Co and Dy-NdFeB crystals we also selected other two ''flower'' patterns, as shown in Figs. 6(a) and 6(b). They were taken from a $NdFe_{10.5}Mo_{1.5}$ thick single crystal[12] and a 60-$\mu$ m-thick garnet bubble film by using NanoScope IIIa magnetic force microscope. After the patterns of Figs. 6(a) and 6(b) were converted to that in dual-value description, their box dimension $D_{box}$ i.e., the saturated dimension $D_{sat}$ were calculated.

As mentioned above, the ''flower'' patterns are developed by a full branching process. Apparently, the ''flowers'' result from the balance of exchange energy and magnetostatic energy. Therefore, $D_{sat}$ should be related to the exchange coupling length $l_{ex}$ of the materials. The definition of $l_{ex}$ is

$$l_{ex}=(2A/\mu_0 M_S^2)^{1/2}. \tag{2}$$

The exchange constant, saturated magnetization, the corresponding $l_{ex}$, and $D_{sat}$ of the above four kinds of crystals are listed in Table I. From the table, it seems that longer $l_{ex}$ is, the higher $D_{sat}$ is.

TABLE I. Exchange constant $A$, saturated magnetization $M_s$, exchange length $l_{ex}$, and saturated dimension $D_{sat}$ of Co (Ref. 13), Dy-NdFeB (Ref. 14), $NdFe_{10.5}Mo_{1.5}$ (Ref. 12) and garnet bubble film (Ref. 15).

| Materials | $A(\times 10^{-12}$ J/m) | $M_s$ (kA/m) | $l_{ex}$ (nm) | $D_{sat}$ |
|---|---|---|---|---|
| Co | 10.3 | 1422 | 2.8 | 1.55 |
| Dy-NdFeB | 7.7 (Ref. 16) | 875 | 4.0 | 1.65 |
| $NdFe_{10.5}Mo_{1.5}$ | 22 | 812 | 7.3 | 1.68 |
| Bubble film | $\sim 1$ | $\sim 16$ | $\sim 79$ | 1.74 |

In conclusion, a fractal study was first introduced into an analysis of two types of ''two-phase'' magnetic domain patterns. The two-phase domain patterns formed under the application of nonlinear fields, or in branching process present fractal nature. The line-measuring dimension $D_{line}$ has been selected to describe the ''line'' structure patterns, such as stripe and plate domains, and the MBD formed in bubble films. For describing the ''plane-filling'' patterns of complicated domains, such as corrugation and spike, even ''flower'' patterns, the box-counting dimension $D_{box}$ has been selected. Finally, a series of domain patterns of Co and Dy-NdFeB single crystals of various thickness $t$ have been described by $D_{line}$ and $D_{box}$ in sections, resulting in a curve of D vs $\log t$. From the curves, the existence of the critical thickness $t_c$ is confirmed; moreover, a saturated dimension $D_{sat}$ is acquired. For different materials, $D_{sat}$ is different, and the correlation seems to be the longer the exchange coupling length $l_{ex}$ is, the higher $D_{sat}$ is.

This project was supported by the National Natural Science Foundation of China, under Grant No. 19674074.

*Author to whom correspondence should be addressed.

[1] B. B. Mandelbrot, *The Fractal Geometry of Nature* (San Francisco, 1982).
[2] T. Vicsek, *Fractal Growth Phenomena*, 2nd ed. (World Scientific, Singapore, 1992).
[3] A. Bunde and S. Havlin, *Fractals and Disordered Systems* (Springer-Verlag, Berlin, 1991).
[4] K. L. Babcock and R. M. Westervelt, Phys. Rev. Lett. **63**, 175 (1989).
[5] K. L. Babcock and R. M. Westervelt, Phys. Rev. Lett. **64**, 2168 (1990).
[6] Zhou Yan, Zheng De-juan, Li Dan, and Han Bao-shan, Chin. Phys. Lett. **17**, 52 (2000).
[7] B. S. Han, J. Magn. Magn. Mater. **100**, 455 (1991).
[8] L. D. Landau, J. Phys. USSR **7**, 99 (1943).
[9] E. Lifshitz, J. Phys. USSR **8**, 337 (1944).
[10] A. Hubert, Phys. Status Solidi **24**, 669 (1967).
[11] A. Hubert and R. Schäfer, *Magnetic Domains* (Springer, New York, 1998).
[12] Xu Hai Han Baoshan, Yang Jinbo, and Yang Yingchang, Sci. China **42**, 94 (1999).
[13] D. J. Craik and R. S. Tebble, *Selected Topics of Solid State Physics Volume IV: Ferromagnetism and Ferromagnetic Domains* (North-Holland, Amsterdam, 1965).
[14] D. Plusa, J. Magn. Magn. Mater. **140-144**, 1061 (1995).
[15] The saturated magnetization is fit to the garnet magnetic bubble films, with about 5-$\mu$m-diameter bubbles. This exchange constant is usually selected for bubble films.
[16] We adopted the exchange constant of sintered NdFeB as that of Dy-NdFeB.